Some Remarks on the Validity of Reynolds Equation in the Modeling of Lubricant Film Flows on the Surface Roughness Scale

T. Almqvist

R. Larsson

Division of Machine Elements,
Luleå University of Technology,
SE-971 87 Luleå, Sweden

The objective of this paper is to investigate the flow in a lubricant film on the surface roughness scale and to compare the numerical solutions obtained by two different solution approaches. This is accomplished firstly by the CFD-approach (computational fluid dynamic approach) where the momentum and continuity equations are solved separately, and secondly the Reynolds equation approach, which is a combination and a simplification of the above equations. The rheology is assumed to be both Newtonian and non-Newtonian. An Eyring model is used in the non-Newtonian case. The result shows that discrepancies between the two approaches may occur, primarily due to a singularity which appears in the momentum equations when the stresses in the lubricant attain magnitudes that are common in EHL. This singularity is not represented by the Reynolds equation. If, however, the rheology is shifted to a non-Newtonian Eyring model the deviations between the two solution approaches is removed or reduced. The second source of discrepancies between the two approaches is the film thickness to wavelength scale ω. It will be shown that the Reynolds equation is valid until this ratio is approximately $O(10^{-2})$. [DOI: 10.1115/1.1760554]

1 Introduction

When modeling in elastohydrodynamic lubrication (EHL), the Reynolds equation is the main partial differential equation to be applied. It was derived by Osborn Reynolds in 1886 [1] and combines the equations of momentum and continuity into a single equation for the fluid pressure. When the derivation is carried out, inertia is neglected due to the small Reynolds number in combination with the thin film in the contact region (see, for example, Khonsari and Booser [2]).

There is no doubt about the validity of this assumption, as long as the region of interest is within the contact and the length scales are large compared to the scales across the fluid film. If, however, ridges or grooves are present, the length to film thickness ratio may be altered and the approximation may be questionable if one studies a local surface roughness irregularity. Asperities with high slope, or short wavelength, may have a characteristic length in the same order of magnitude as the local film thickness. Therefore, it is important to investigate if Reynolds' equation is valid in modeling and simulation of the lubrication between real (rough) surfaces. If the film cannot be seen as very thin it is possible that flow components and pressure differences may appear across the lubricating film.

In a CFD (computational fluid dynamics) approach on the other hand, the momentum and continuity equation is used in their basic form, which means no assumptions about neglecting inertia or approximations due to thin lubricating films are used. With such an approach the physics of the flow is retained in a more complete way and makes it possible to investigate the validity of the approximations made in the traditional solution approach, i.e., the Reynolds equation approach.

It has been shown earlier by the authors [3,4] that it is possible to use commercial CFD-software to simulate EHL in line contacts. Both thermal and isothermal analyses of the smooth surface problem were presented. Schäfer [5] used a CFD approach to solve the Stokes equations (the Navier-Stokes equations without inertia terms) to solve the EHL line contact problem. That investigation points out that significant pressure differences across the lubricating film can occur in EHL when a high degree of sliding is present. However, the shear stresses in the lubricant film became remarkably high and the CFD-approach may run into trouble when the (principal) stresses in the fluid become too high. Renardy [6] and Bair et al. [7] showed that a singularity might appear in the momentum equation at high shear stresses. It was speculated that the singularity is the driving force behind the mechanical shear bands observed in their experimental investigations at high shear rate.

The high shear stresses in EHL occur due to the strong pressure dependency of viscosity in combination with high shear rates. If the singularity is reached, the momentum equation undergoes a change of type, and non-existence and non-uniqueness may occur (see Renardy [6]). If the momentum equation is not valid under such circumstances, it is also questionable whether the Reynolds equation is valid.

The validity of the Reynolds equation has been discussed recently by Odyck and Venner [8]. They investigated the differences between Stokes and Reynolds equations under isoviscous, Newtonian and incompressible conditions. They found large differences between the Reynolds and Stokes equations in predicted load when the film thickness to wavelength ratio is $O(0.1)$.

This investigation will give more clarity about the validity of the Reynolds equation for the modeling of EHL under Newtonian, non-Newtonian, piezoviscous and compressible conditions. The following issues will be discussed:

- Can any differences be observed between the Reynolds equation approach and the CFD-approach when the film thickness to wavelength scale ω is altered? The strategy here is to investigate where the limit of the Reynolds equation appear, i.e., is Reynolds equation valid also for cases where the characteristic length of the film is almost as small as the film thickness?
- How does the singularity in the momentum equation affect

Contributed by the Tribology Division for publication in the ASME JOURNAL OF TRIBOLOGY. Manuscript received by the Tribology Division July 1, 2003; revised manuscript received March 25, 2004. Associate Editor: C. H. Venner.

the numerical solution when surface roughness flows are simulated? Are there any discrepancies between the Reynolds equation and the CFD-solutions due to the singularity?

- Is it possible to modify the CFD-code to take an Eyring rheology into account? A non-Newtonian rheology such as the one described by the Eyring model will reduce the stresses in the film and may therefore prevent the occurrence of the singularity in the momentum equations.
- How do discrepancies between the CFD and Reynolds equation approaches respond to a shift to Eyring rheology?
- Are there any pressure differences across the lubricant film when surface roughness is present?

The geometries used in the investigations are two-dimensional geometries with a single ridge located at a stationary surface. No deformations are allowed and the boundary conditions are periodic, so, the geometry can be thought of as an isolated surface asperity, already deformed, within an EHL line contact.

2 Governing Equations

The governing equations for the CFD approach are the equations of momentum and continuity (see CFX 4.4 [9]). The stationary momentum (no body forces) equation

$$\nabla\cdot(\rho\mathbf{u}\otimes\mathbf{u})=\nabla\cdot\sigma \tag{1}$$

The density is denoted by ρ and $\mathbf{u}$ is the velocity field. The symbol σ denotes the total stress tensor and the symbol $\otimes$ denotes the vector product $u_i\times u_j$.

The stationary equation of continuity reads

$$\nabla\cdot(\rho\mathbf{u})=0 \tag{2}$$

The total stress tensor is

$$\sigma=-p\,\delta+\tau \tag{3}$$

where p, δ denote the pressure and unit tensor, τ is the dynamic part of the stress tensor. The bulk viscosity is neglected with the aid of Stokes assumption and the dynamic stress tensor, for a Newtonian fluid, reads

$$\tau=-\frac{2\eta}{3}\nabla\cdot\mathbf{u}\delta+\eta\{\nabla\mathbf{u}+(\nabla\mathbf{u})^T\} \tag{4}$$

where the dynamic viscosity is denoted by η. When a non-Newtonian Eyring model is used, a generalized viscosity μ derived from the Eyring equation replaces the viscosity η

$$\mu=\frac{\tau_0}{\dot\gamma}\sinh^{-1}\left(\frac{\eta\dot\gamma}{\tau_0}\right) \tag{5}$$

where τ_0 is the stress where the nonlinear fluid flow behavior begins, i.e., the Eyring stress, and $\dot\gamma$ is the rate of deformation tensor. The form of Reynolds equation used in this work is proposed by Conry et al. [10] and reads

$$\frac{d}{dx}\left\{\frac{\rho h^3}{12\eta}\frac{dp}{dx}S(x)\right\}=\frac{u_1+u_2}{2}\frac{d(\rho h)}{dx}$$
$$S(x)=\frac{3(\Sigma\cosh\Sigma-\sinh\Sigma)}{\Sigma^3}\sqrt{1+\frac{\eta^2(u_2-u_1)^2}{(\tau_0 h)^2}\frac{\Sigma^2}{\sinh^2\Sigma}} \tag{6}$$
$$\Sigma=\frac{h}{2\tau_0}\frac{\partial p}{\partial x}$$

The film thickness is denoted by h and u_1, u_2 are the surface velocities. The non-Newtonian factor, S, is defined according to Johnson and Tevaarwerk [11].

The expression for the viscosity is the Roelands expression and reads [12]

$$\eta(p)=\eta_0\exp\left\langle(\ln\{\eta_0\}+9.67)\left(-1+\left\{1+\frac{p}{p_0}\right\}^z\right)\right\rangle \tag{7}$$

where η_0 denotes the viscosity at atmospheric pressure, p_0 is a constant and z is the pressure-viscosity index.

The expression used for the density is the Dowson-Higginson expression [13]

$$\rho(p)=\rho_0\frac{(C_1+C_2p)}{(C_1+p)} \tag{8}$$

where the density at atmospheric pressure is denoted by ρ_0. C_1 and C_2 are constants. The asperity ψ is modelled by the following expression

$$\psi(x)=A\times10^{[-10\{(x-x_c)/\lambda\}^2]}\cos\left\{\frac{2\pi(x-x_c)}{\lambda}\right\} \tag{9}$$

where A is the amplitude, x_c is the position of the center of the ridge and λ is the wavelength.

2.1 The Thin Film Approximation. The source of deviations between the Reynolds and the momentum equation is due to the simplifications made in the momentum equation. In order to discuss the differences, a scaled momentum equation is presented. The equations showed here are limited to two-dimensional with a Newtonian or generalized Newtonian behavior. The variables denoted with an overbar are dimensionless, and the corresponding characteristic parameters are denoted by a subscript (r).
The scaled momentum equations read

$$\mathrm{Re}_m\overline{\rho u}\frac{\partial\overline{u}}{\partial\overline{x}}+\mathrm{Re}_m\overline{\rho v}\frac{\partial\overline{u}}{\partial\overline{y}}=-\frac{\partial\overline{p}}{\partial\overline{x}}+\frac{4\omega^2}{3}\frac{\partial}{\partial\overline{x}}\overline{\mu}\frac{\partial\overline{u}}{\partial\overline{x}}-\frac{2\omega^2}{3}\frac{\partial}{\partial\overline{x}}\overline{\mu}\frac{\partial\overline{v}}{\partial\overline{y}}+\frac{\partial}{\partial\overline{y}}\overline{\mu}\frac{\partial\overline{u}}{\partial\overline{y}}+\omega^2\frac{\partial}{\partial\overline{y}}\overline{\mu}\frac{\partial\overline{v}}{\partial\overline{x}}$$
$$\mathrm{Re}_m\overline{\rho u}\frac{\partial\overline{v}}{\partial\overline{x}}+\mathrm{Re}_m\overline{\rho v}\frac{\partial\overline{v}}{\partial\overline{y}}=-\frac{1}{\omega^2}\frac{\partial\overline{p}}{\partial\overline{y}}+\omega^2\frac{\partial}{\partial\overline{x}}\overline{\mu}\frac{\partial\overline{v}}{\partial\overline{x}}+\frac{\partial}{\partial\overline{x}}\overline{\mu}\frac{\partial\overline{u}}{\partial\overline{y}}+\frac{4}{3}\frac{\partial}{\partial\overline{y}}\overline{\mu}\frac{\partial\overline{v}}{\partial\overline{y}}-\frac{2}{3}\frac{\partial}{\partial\overline{y}}\overline{\mu}\frac{\partial\overline{u}}{\partial\overline{x}} \tag{10}$$
$$\mathrm{Re}_m=\frac{\rho_r u_r x_r\omega^2}{\eta_r},\qquad\omega=\frac{y_r}{x_r}$$

In these equations x_r, y_r are the characteristic length scales along the across the film and μ_r is the reference viscosity. The pressure is made nondimensional by the ratio $\mu_r u_r x_r/y_r^2$. The ratio y_r/x_r is denoted by ω and the modified Reynolds number in the x and y-directions is denoted by Re_m.

The velocity in the x-direction is denoted by u_r and the velocity across the film is scaled as $v_r=u_r\omega$. As can be observed, assuming small values of ω leads to the starting point of the derivation of the Reynolds equation; hence the simplified momentum equations

$$\frac{\partial\overline{p}}{\partial\overline{x}}=\frac{\partial}{\partial\overline{y}}\overline{\mu}\frac{\partial\overline{u}}{\partial\overline{y}}$$
$$\frac{\partial\overline{p}}{\partial\overline{y}}=0 \tag{11}$$

From the equations in (10) it can further be observed that, if the ratio ω increases, more terms in the equilibrium equations will be important. This results in deviations between the CFD and the Reynolds equation approach when predicting the fluid pressure. The viscosity variations along the fluid film may also introduce discrepancies between the two approaches. The generalized viscosity μ in the Eyring model will be influenced by variables such as the viscosity η, shear rate $\dot\gamma$ and the Eyring stress τ_0.

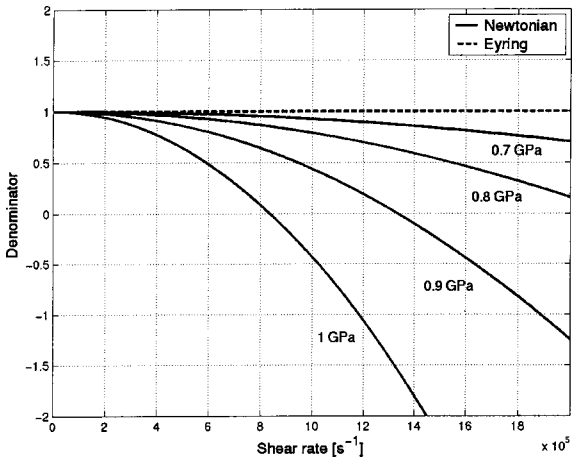

Fig. 1 The denominator in the modified momentum equations for Newtonian (-) and Eyring (--) rheological models. The pressure is denoted beside the curves.

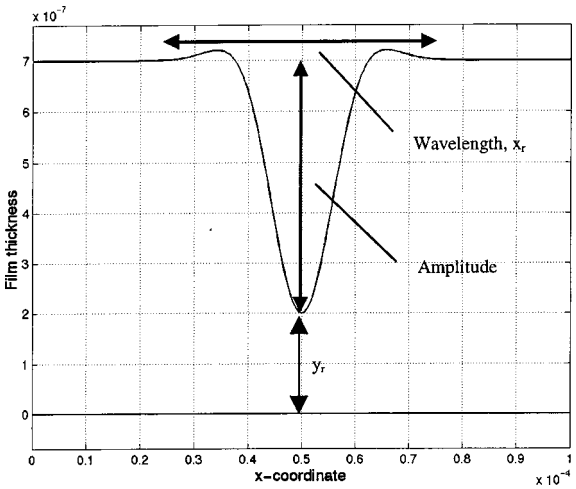

Fig. 2 Ridge geometry

3 The Singularity

The influence of the singularity in EHL applications has been discussed earlier by Almqvist and Larsson [3,4] and Bair et al. [7]. In order to discuss and investigate the appearance and influence of the singularity, the modified momentum equations will be presented below. The assumptions behind the derivation of these modified momentum equations are

- No body forces
- No compressibility
- Isothermal conditions
- No inertia forces

A rewriting of the momentum equation (1) in addition to the assumptions above will now give the following modified momentum equations for the contact region, here expressed in Cartesian components

$$\frac{\partial p}{\partial x} = \frac{2\mu\mu' e_{xy}\nabla^2 v + (1-2\mu' e_{yy})\mu\nabla^2 u}{1-(2\mu')^2(e_{xy}^2 - e_{xx}e_{yy})}$$

$$\frac{\partial p}{\partial y} = \frac{2\mu\mu' e_{xy}\nabla^2 u + (1-2\mu' e_{xx})\mu\nabla^2 v}{1-(2\mu')^2(e_{xy}^2 - e_{xx}e_{yy})} \tag{12}$$

The rate of deformation tensor, e_{ij}, is defined as

$$e_{ij} = \frac{1}{2}\left(\frac{\partial u_i}{\partial x_j} + \frac{\partial u_j}{\partial x_i}\right) \tag{13}$$

The derivative of viscosity with respect to pressure is denoted by μ'. As can be observed, there will be a singularity in the momentum equations if the denominator approaches zero and the nominator is different from zero. In the numerical simulations, it will be important to check whether the denominator in the momentum equations affects the CFD-solution. That will help us to judge if the differences between the Reynolds and the CFD-solutions are due to the thin film approximation or the singularity. The singularity is actually also a result of the approximation of thin lubricating films, but there may be differences between the two approaches even if the vicinity of the singularity is not reached. This is the reason for the distinction between the two sources of error.

Figure 1 shows the value of the denominator for the modified momentum equations (12) and its variation with shear rate. Viscosity is assumed to be the only pressure dependent variable when the denominator by adopting the Eyring model. This is not completely true; both the Eyring stress τ_0 and the pressure-viscosity coefficient z depend on pressure. But, in the range of the pressures investigated in the numerical simulations, the dependency is small so the approximation is assumed to be reasonable (see Evans and Johnson [14], Bair et al. [7]).

The value of the viscosity at ambient pressure is set to 0.1 Pa s and the Eyring stress to 7 MPa. The pressure viscosity index is set to 0.4 and, according to Fig. 1; the assumption of Newtonian rheology will give an upper limit for the shear rate and pressure. If care is not taken, the denominator will pass through zero. If, for example, the shear rate is 8×10^6 s^{-1}, the maximum pressure is approximately 1 GPa.

In the CFD-solution, a passage through zero will lead to a rapid divergence in the numerical simulation (Renardy [6]). In Fig. 1, the dashed line is composed of four different curves (at different pressures) when Eyring rheology is used, and with the parameters used here, it is not likely that the denominator influences the numerical solution.

4 Numerical Solution

The full equations of momentum and continuity were solved numerically by the use of the CFD-code CFX4.4 [9]. The expressions for the viscosity and density had to be implemented in the user routines USRVIS and USRDEN.

The code uses a finite volume discretisation of second order accuracy in the diffusive terms and hybrid discretisation for the convective terms. (The code switches between a first and second-order discretization when the local Peclet number exceeds 2.) Because of the dominance of the diffusive terms in the contact region in EHL-conjunctions, the scheme is assumed to be of second-order accuracy.

The pressure correction algorithm was SIMPLE. The relaxation algorithm for the momentum equations was Stone's method, for the pressure correction Stone's and ICCG (pre-conditioned conjugated gradient method), see CFX4.4 [9]. The meshes used in the simulations were structured and uniform.

5 Results

In this chapter the results of the numerical simulations are shown. The geometry is chosen to be a single ridge, see Fig. 2, and is located at the upper stationary surface. The flat lower surface is moving with a constant velocity U. The surfaces throughout the simulations were assumed to be rigid (no elastic deformations were allowed).

The boundary conditions are periodic and the ambient pressure level in the simulations was adjusted through an ambient pressure P_{amb}. Such an approach is adopted to resemble the influence of a ridge on the fluid flow in a real EHL-contact, where the surrounding pressure is high.

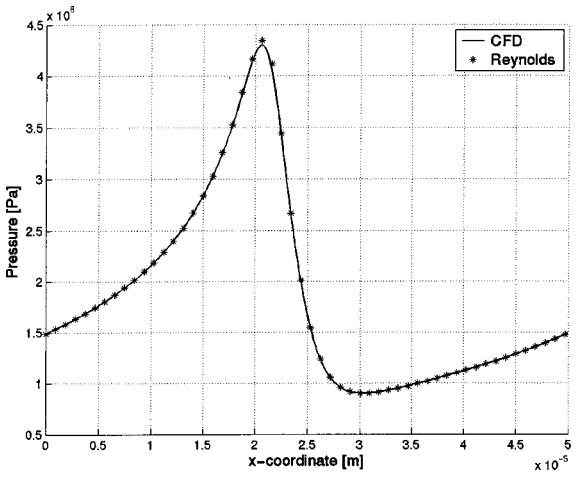

Fig. 3 Pressure distribution for the two approaches when a Newtonian rheology is used. The CFD-solution denoted by (-) and the Reynolds solution by (*), $\omega = 2.5\times10^{-3}$.

In the CFD-approach the field variables have also a resolution across the film and when comparisons between the two approaches are made, the field variable (pressure) is taken from a trace in the middle of the film.

5.1 The Singularity. In the first experiments, a numerical validation of the two approaches was performed. The ratio ω is taken as 2.5×10^{-3}. The rheology is assumed to be Newtonian and the result is shown in Fig. 3. The parameters used in the simulations are contained in test case 1, Table 1. As can be observed, the solution for the fluid pressure predicted by the CFD and Reynolds equation correspond very well which is expected when the ratio ω is $O(10^{-3})$. The maximum deviation between the two approaches is 1.3% and is probably due to the mesh resolution (the maximum discretisation error in the CFD-solution is 1.3%).

The discretization errors through the simulations are contained in Table 2, and in the CFD-case computed along a trace in the middle of the fluid film. The discretisation error is the ratio of the maximum discretisation error and the maximum pressure.

In the next experiment, test case 2, Table 1, the ambient pressure was adjusted to increase by 0.01 GPa. The impact in the numerical experiments can be studied in Fig. 4. The strategy was to force the denominator in the modified momentum equations (12) towards zero. Care must be taken here to avoid a passage through the singularity. The ratio ω is the same as in the above case and, as can be observed, the CFD-solution predicts a higher pressure compared to the Reynolds equation solution.

If one forces the solution closer to the singularity, even larger discrepancies will occur. The maximum deviation in pressure between the two solutions is approximately 17%. So, when Newtonian rheology is assumed, there may be large deviations between the two approaches. The pressure increase is higher in the CFD-solution because of the influence of the singularity in the modified momentum equations (12). The denominator in the modified momentum equations is approximately 0.4, see Fig. 1.

The next experiment, test case 3, Table 1, involves an investigation carried out to examine how the singularity responds to a change in the rheological model. The viscosity in the CFD-code is now modified to take a generalized Newtonian model into account, where the Eyring model was chosen. The parameters used

Table 1 Parameters for the singularity investigation

PARAM.	TEST CASE 1.	TEST CASE 2.	TEST CASE 3.	TEST CASE 4.	DIMENSION
ρ_0	870	870	870		kg m^{-3}
η_0	0.1	0.1	0.1	0.1	Pa s
U	0.2	0.2	0.2		m s^{-1}
Z	0.4	0.4	0.4	0.7	-
P_{amb}	0.15	0.16	0.16		GPa
x_r	40	40	40		μm
y_r	0.1	0.1	0.1		μm
H	0.2	0.2	0.2		μm
τ_0	-	-	7	10, 20, 40	MPa

Table 2 Error estimates and meshes

TEST CASE	$\varepsilon_{d\,\max}$, CFD REYNOLDS %	ε_C CFD REYNOLDS %	MESH CFD	MESH REYNOLDS
1.	1.3/0.79	$10^{-4}/10^{-3}$	400×20×1	800
2.	5.2/1.2	$10^{-4}/10^{-4}$	800×40×1	1600
3.	0.31/0.59	$10^{-4}/10^{-4}$	800×40×1	800
5. $y_r=4*10^{-7}$ m$\omega=1/3$	$1.6\times10^{-3}/2.4\times10^{-3}$	$10^{-3}/10^{-2}$	400×20×1	800
5. $y_r=4*10^{-7}$ m$\omega=0.1$	$3.6\times10^{-3}/7.8\times10^{-3}$	$10^{-5}/10^{-2}$	400×20×1	800
5. $y_r=4*10^{-7}$ m$\omega=0.01$	0.035/0.073	$10^{-5}/10^{-2}$	400×20×1	800
5. $y_r=4*10^{-7}$ m, $\omega=0.001$	0.047/0.066	$10^{-5}/10^{-2}$	400×20×1	800
5. $y_r=1*10^{-7}$ m, $\omega=1/3$	0.31/0.014	$10^{-3}/10^{-3}$	400×20×1	800
5. $y_r=1*10^{-7}$ m, $\omega=0.1$	0.043/0.044	$10^{-3}/10^{-3}$	400×20×1	800
5. $y_r=1*10^{-7}$ m, $\omega=0.01$	0.15/0.37	$10^{-5}/10^{-3}$	400×20×1	800
5. $y_r=1*10^{-7}$ m, $\omega=0.001$	0.34/0.52	$10^{-5}/10^{-3}$	400×20×1	1600
5. $y_r=5*10^{-8}$ m, $\omega=1/3$	1.8/0.018	$10^{-5}/10^{-3}$	800×40×1	800
5. $y_r=5*10^{-8}$ m, $\omega=0.1$	0.25/0.061	$10^{-4}/10^{-3}$	400×20×1	800
5. $y_r=5*10^{-8}$ m, $\omega=0.01$	0.21/0.52	$10^{-4}/10^{-3}$	400×20×1	800
5. $y_r=5*10^{-8}$ m, $\omega=0.001$	0.20/0.83	$10^{-5}/10^{-2}$	400×20×1	1600
6. $y_r=5*10^{-8}$ m, $P_{\text{amb}}=0.1$ GPa	0.035/0.032	$10^{-3}/10^{-3}$	400×20×1	800
6. $y_r=5*10^{-8}$ m, $P_{\text{amb}}=0.3$ GPa	0.087/0.054	$10^{-3}/10^{-3}$	400×20×1	800
6. $y_r=5*10^{-8}$ m, $P_{\text{amb}}=0.5$ GPa	0.25/0.061	$10^{-4}/10^{-3}$	400×20×1	800
6. $y_r=5*10^{-8}$ m, $P_{\text{amb}}=0.75$ GPa	0.44/0.057	$10^{-5}/10^{-3}$	400×20×1	800
6. $y_r=5*10^{-8}$ m, $P_{\text{amb}}=1$ GPa	0.57/0.053	$10^{-3}/10^{-3}$	400×20×1	800

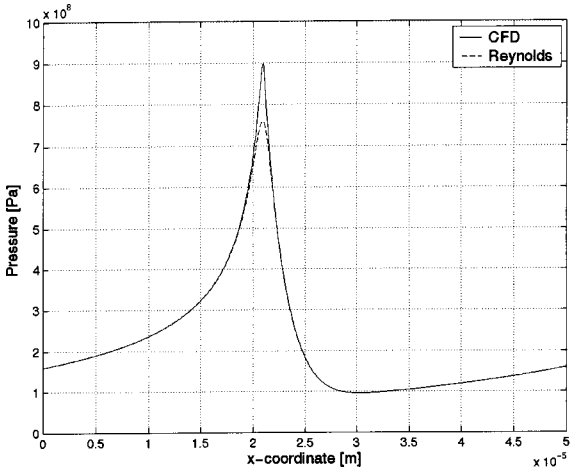

Fig. 4 The CFD-solution (-) compared with the Reynolds equation solution (--) when the singularity influences the solution. The rheology is assumed to be Newtonian, $\omega = 2.5 \times 10^{-3}$.

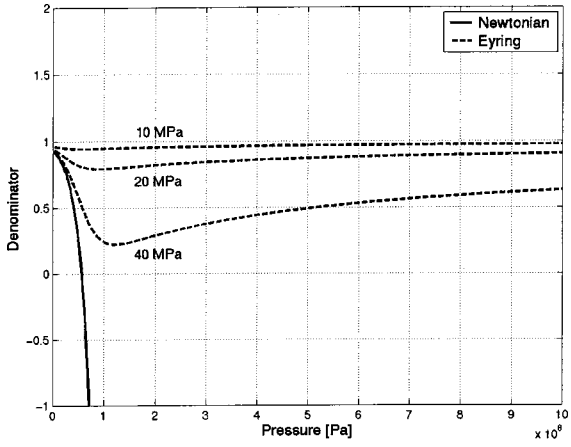

Fig. 6 The denominator in the modified momentum equations for a Newtonian (-) and an Eyring (--) rheological model. The Eyring stress τ_0 is denoted beside the curves.

in this experiment are the same as those in test case 2, apart from the Eyring model for the generalized viscosity μ.

The results from the CFD and Reynolds equation simulations can be seen in Fig. 5, and as can be observed, the two approaches predict the same fluid pressure. The reason for this behavior is that the Eyring model influences the principal stresses to exhibit a weaker dependence in shear rate (see Fig. 1) and the vicinity of the singularity is not reached as in the previous simulation where Newtonian rheology was assumed.

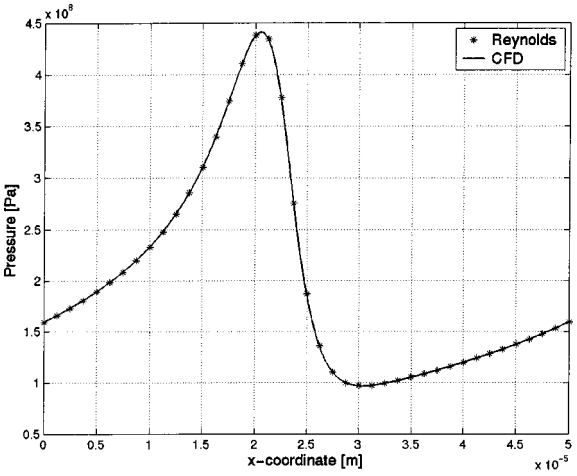

Fig. 5 The CFD and Reynolds equation solution for an Eyring rheological model, $\omega = 2.5 \times 10^{-3}$

So, the question will then be: Is the singularity a result from a naive use of the Newtonian model, or can the singularity be of importance even if the rheology follows an Eyring model? To answer that question, an investigation, test case 4, Table 1, was performed in order to see if the model removed or delayed the influence of the singularity. To do that, some estimates of the physical parameters used in the model were performed. Higher values of the pressure-viscosity coefficient, shear rate and Eyring stress will force the denominator in the modified momentum equations (12) towards zero. Three different values of Eyring stress were used. The values were 10, 20, and 40 MPa. The value of the pressure viscosity index was set to 0.7 (correspond to $\alpha = 2.6 \times 10^{-8}$) and the shear rate to 10^8 s^{-1}.

As can be observed in Fig. 6, there is Newtonian behavior in the region of low pressure and Eyring behavior when the pressure is increased. From this experiment conclusions may be drawn that a shift to an Eyring model reduces or removes the influence of the singularity. In the case of an extremely high Eyring stress, some influence is however expected.

5.2 The Thin Film Approximation. The next subject was to investigate how the two approaches respond on scale changes in the ridge geometry, i.e., the error in the thin film approximation. The parameters used in the simulations are contained in Table 3. The rheology was assumed to be of Eyring type through out the simulations, and the varied geometrical parameters were the ratio ω and the minimum film thickness y_r (for the simulation where the ratio $\omega = 10^{-3}$ the ambient viscosity is decreased due to the extremely high pressure obtained).

The maximum pressure deviation between the two approaches is shown in Fig. 7. The maximum deviation is presented as the ratio between deviation and the maximum pressure in the domain. From the simulations, it can be observed that the Reynolds equa-

Table 3 Parameters for the film thickness to the wavelength investigation

PARM.	$\omega = 1/3$	$\omega = 0.1$	$\omega = 0.01$	$\omega = 10^{-3}$	-
ρ_0	870	870	870	870	kg m^{-3}
η_0	0.1	0.1	0.1	0.02	Pa s
U	0.2	0.2	0.2	0.2	m s^{-1}
Z	0.4	0.4	0.4	0.4	-
P_{amb}	0.5	0.5	0.5	0.5	GPa
y_r	0.4, 0.1, 0.05	0.4, 0.1, 0.05	0.4, 0.1, 0.05	0.4, 0.1, 0.05	μm
H	0.5	0.5	0.5	0.5	μm
τ_0	7	7	7	7	MPa

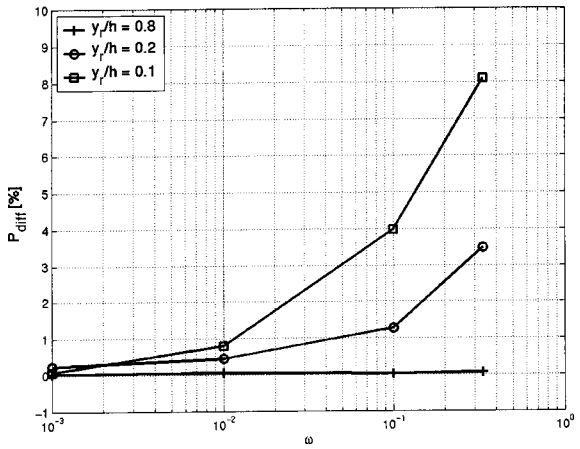

Fig. 7 The ratio of the maximum deviation between the CFD and Reynolds equation and the maximum pressure. In the figure, three different ratios y_r/h are shown versus ω.

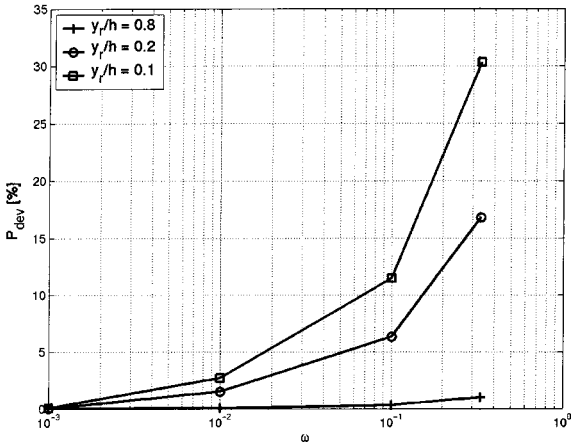

Fig. 9 The ratio of the maximum pressure difference across the fluid film and the maximum pressure along a trace in the middle of the film in the CFD-computations. In the figure, three different ratios y_r/h are shown versus ω.

tion is still a good approximation when the ratio ω is $O(10^{-2})$. When the ratio reaches $O(10^{-1})$, the approximation becomes more insecure and the deviations will grow even further when the gap between the nip of the asperity and the lower boundary decreases.

The reason for such behavior is that a decrease in y_r will increase the shear rate and the viscosity μ will have a large content of shear thinning in the region of the nip. That will increase the influence of the diffusive terms in the momentum equations containing derivatives along the fluid film, see Eq. (10).

Figure 8 shows the results from an investigation carried out in order to clarify how the ambient pressure influences the differences between the two approaches. The parameters used in the simulations are contained in Table 4. The pressure level P_{amb} is adjusted in the range 0.1–1.0 GPa. One can see from Fig. 8 that when the ambient pressure is increased the difference between the two approaches grows but has a reduced gradient. This behavior occurs due to the Eyring model. When the fluid pressure is high, shear-thinning behavior occurs in the whole domain and a further increase in the pressure will not cause any larger deviations in the generalized viscosity μ. The diffusive terms neglected in the momentum equation in the Reynolds approach will now have a weaker influence due to the reduced longitudinal change in the viscosity.

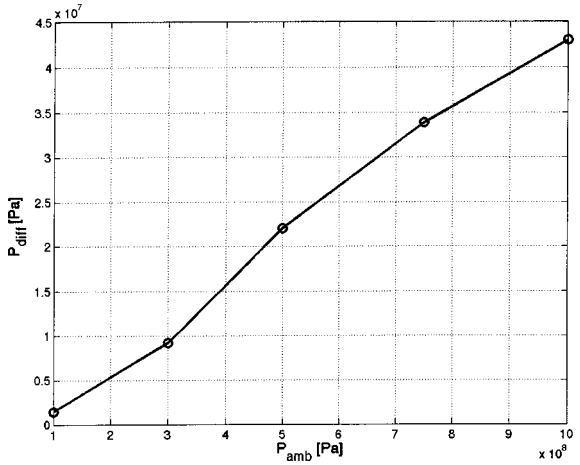

Fig. 8 The deviation in pressure between the CFD and Reynolds equation approaches versus ω. The ratio y_r/h is held to a constant value $y_r/h=0.1$.

The final results in this investigation are the pressure variation across the fluid film. The parameters used are contained in Table 3. As expected, the pressure differences across the fluid film will change when the ratio ω increases. The results shown in Fig. 9 are the ratio between maximum pressure deviation across the fluid film and the maximum pressure along a trace in the middle of the film. So, when the ratio ω increases above $O(10^{-2})$, it is necessary to include the momentum equation in the y-direction in order to be able to resolve the pressure differences across the fluid film.

6 Discussion

The numerical experiments that have been carried out in this work are greatly simplified in order to investigate the small-scale lubricant flow in EHL. It is, however, interesting to note that the validity of the Reynolds equation is still good if the ω-ratio decreases to $O(10^{-2})$. A common assumption in the derivation of the Reynolds equation is that the scales along the fluid film are three orders of magnitude larger than the scale across the fluid film. When the above mentioned ratio grows further, the deviation (between the two approaches) in fluid pressure increases both

Table 4 Parameters for the ambient pressure investigation

PARAM.	$P_{amb}=0.1$	$P_{amb}=0.3$	$P_{amb}=0.5$	$P_{amb}=0.75$	$P_{amb}=1$	GPa
ρ_0	870	870	870	870	870	kg m^{-3}
η_0	0.1	0.1	0.1	0.02	0.02	Pa s
U	0.2	0.2	0.2	0.2	0.2	m s^{-1}
z	0.4	0.4	0.4	0.4	0.4	-
P_{amb}	0.5	0.5	0.5	0.5	0.5	GPa
y_r	0.05	0.05	0.05	0.05	0.05	μm
h	0.5	0.5	0.5	0.5	0.5	μm
τ_0	7	7	7	7	7	MPa

along and across the fluid film. Here it may also be necessary to separate the computation of the elastic deformations on the surfaces due to the deviation in pressure distribution on the upper and lower surfaces, i.e., the upper and lower surfaces may deform differently and may result in thinner film than expected.

In real EHL-applications, the asperities will change due to elastic deformations but if the lubricant has a shear thinning or limiting stress behavior, the local pressure increase is not high enough to flatten out the asperities. Hence, much of the asperities will travel through the conjunctions without any larger deformations due to a poor local pressure generation effect.

The reduction in local pressure due to the shear thinning behavior also has the effect that deviations between the two approaches compared to the surrounding pressure are limited. That means that the differences would probably be more pronounced with a Newtonian rheological model assumption. So, a change to Eyring rheology prolongs the validity of the Reynolds equation compared to a Newtonian case.

The deviations between the CFD and Reynolds equation may also be governed by a singularity in the momentum equations (12). If the lubricant sustains shear stresses in the neighborhood of the singular value (Newtonian or non-Newtonian rheology), it is clear that the pressure predicted by the CFD-approach is increased compared to Reynolds equation approach. Bair et al. [7] suggest that the singularity in the momentum equation might be the source of the mechanical shear band seen in their experiments. This investigation does not, however, support such theory since the singularity cannot be reached with a shear thinning model.

One has also to bear in mind that the computations made here are based on isothermal theory and the temperature rise in the lubricant will also influence the stresses in the lubricant. An increase of the temperature results in a reduction in viscosity and stresses in the fluid are reduced.

Finally, the number of mesh elements on the ridge must be very large in order to resolve the physics with satisfactorily. Approximately 100 elements per surface irregularity seems to be a reasonable mesh resolution. If one tries to resolve the pressure peak in test case 2, Table 1, the number of CVs/elements is an order of magnitude larger. That raises questions about simulations with real surfaces, where it is clear that; if one wants to resolve the problem on the roughness scales fully, very powerful computations are necessary.

7 Conclusions

The aim of this work was to investigate if Reynolds equation is valid in the modelling of rough surface elastohydrodynamic lubrication. The traditional way of simulating the lubricant flow by the Reynolds equation was compared with the less approximating CFD-approach and the results from the numerical simulations show that:

- The ratio ω must of be $O(10^{-2})$ or greater in order to show any larger discrepancies between the two approaches due to the error in the thin film approximation. In the simulations performed in this work a ratio $\omega \leqslant 10^{-2}$ gives errors of less than 3% between the two approaches.
- The singularity in the momentum equation may result in a higher pressure in the CFD-solution compared with the Reynolds equation solution if the rheology is assumed to be Newtonian.
- The investigation of the singularity when the Eyring model is used shows that it is not likely that it is possible to force the momentum equation through the singularity. It is more likely that the influence of the singularity will be removed or reduced.
- It is possible to modify the CFD-code to take an Eyring rheological model into account.
- The pressure differences across the fluid film increase as the ratio ω increases. The assumption of neglecting pressure deviation across the lubricating film becomes questionable when the ratio $\omega \geqslant 10^{-2}$.

Acknowledgment

The authors gratefully acknowledge the financial support from the Swedish Research Council (VR) and The National Graduate School in Scientific Computing (NGSSC).

Nomenclature

$\mathbf{u}\ (u,v,w)$ = velocity field, $\mathrm{m\,s^{-1}}$
$u_1,\ u_2$ = surface velocities, $\mathrm{m\,s^{-1}}$
ρ = density, $\mathrm{kg\,m^{-3}}$
ρ_0 = density at ambient pressure, $\mathrm{kg\,m^{-3}}$
σ = total stress tensor, Pa
P = pressure, Pa
μ = generalized viscosity, Pa s
η = dynamic viscosity, Pa s
η_0 = dynamic viscosity at ambient pressure, Pa s
x_c = position of the ridge or groove, m
e_{ij} = rate of deformation tensor, $\mathrm{s^{-1}}$
τ = dynamic stress tensor, Pa
τ_0 = eyring stress, Pa
Re_m = modified Reynolds number, Pa
S = non-Newtonian slip factor
Σ = dimensionless function
h = film thickness, m
P_0 = constant, Pa
z = pressure viscosity coefficient
C_1 = constant, Pa
C_2 = constant
A = amplitude, m
λ = wavelength, m
μ' = derivative with respect to pressure, s
ψ = asperity function, m
$\dot{\gamma}$ = rate of deformation tensor, $\mathrm{s^{-1}}$
ω = film thickness to wavelength ratio
$\varepsilon_{d\,\max}$ = maximum discretisation error
ε_c = convergence error

Sub-superscripts

r = reference parameter
$-$ = dimensionless variables

References

[1] Reynolds, O., 1886, ''On the Theory of Lubrication and Its Application to Mr. Beauchamps Tower's Experiments, Including an Experimental Determination of the Viscosity of Olive Oil,'' Philos. Trans. R. Soc. London, **177**, pp. 157–234.

[2] Khonsari, M. M., and Booser, E. R., 2001, *Applied Tribology*, John Wiley & Sons, New York.

[3] Almqvist, T., and Larsson, R., 2001, ''The Navier-Stokes Approach for Thermal EHL Line Contact Solutions,'' Tribol. Int., **35**, pp. 163–170.

[4] Almqvist, T., and Larsson, R., 2001, ''Comparison of Reynolds and Navier-Stokes Approaches for Solving Isothermal EHL Line Contacts,'' *Proceedings of the WTC Conference*.

[5] Schäfer, C. T., Giese, P., Rowe, W. B., and Woolley, N. H., 1999, ''Elastohydrodynamically Lubricated Line Contact Based on the Navier-Stokes Equations,'' *Proceedings of the 26th Leeds-Lyon Symposium on Tribology*, pp. 57–59.

[6] Renardy, M., 1986, ''Some Remarks on the Navier-Stokes Equations With a Pressure-Dependent Viscosity,'' Commun. Partial Differ. Equ., **11**, pp. 779–793.

[7] Bair, S., Khonsari, M., and Winer, W. O., 1998, ''High-Pressure Rheology of Lubricants and Limitations of the Reynolds Equation,'' Tribol. Int., **31**, pp. 573–586.

[8] Odyck, D. E. A., and Venner, C. H., 2003, ''Stokes Flow in Thin Films,'' ASME J. Tribol., **125**, pp. 121–134.

[9] *CFX 4.4 USER GUIDE*, 1999, AEA Technology.
[10] Conry, T. F., Wang, S., and Cusano, C., 1987, ''A Reynolds Equation for Elastohydrodynamic Lubrication in Line Contacts,'' Transactions of the ASME, **109**, pp. 648–658.
[11] Johnson, K. L., and Tevaarwerk, J. L., 1977, ''The Shear Behavior of Elasto hydrodynamic Oil Films,'' Proc. R. Soc. London, Ser. A, **356**, pp. 215–236.
[12] Roelands, C. J. A., 1966, ''Correlational Aspects of the Viscosity-Temperature-Pressure Relationships of Lubricating Oils,'' Ph.D thesis, Druck, V. R. B., Groningen.
[13] Dowson, D., and Higginson, G. R., 1966, *Elasto-Hydrodynamic Lubrication: The Fundamentals of Roller or Gear Lubrication*, Pergamon Press, Oxford.
[14] Evans, C. R., and Johnson, K. L., 1986, ''The Rheological Properties of Elastohydrodynamic Lubricants,'' Proc. Inst. Mech. Eng., **200**, pp. 303–312.